Resonance-Assisted Hot Electron Femtochemistry at Surfaces

J. W. Gadzuk

National Institute of Standards and Technology, Gaithersburg, Maryland 20899
(Received 27 October 1995)

A theory of resonance-assisted, hot-electron-induced femtochemical processing at surfaces (HEFATS) has been developed in terms of inelastic electron scattering via negative-molecular-ion shape resonances associated with molecules adsorbed on solid surfaces. Two examples, one involving a broad band of laser-excited hot electrons and the other a tunable narrow band produced by a solid state tunnel junction, are used to illustrate the potential of HEFATS in chemical bond breaking as, for instance, in desorption. [S0031-9007(96)00299-2]

The phenomenon of laser-induced, hot electron photochemistry of atoms or molecules adsorbed on solid surfaces has provided a most exciting fundamental area of inquiry in contemporary surface dynamics [1]. It has guided us to the threshold of surface femtochemistry [1(a),2], an emerging field which is based on our ability to control elementary chemical processes at surfaces on the ultrafast time scale of femtoseconds. The essential observations [1] which have stimulated the idea of hot electron photochemistry (dissociation and/or desorption) have been strongly suggestive of a bond-breaking mechanism in which the initial step of the process involves photoexcitation of substrate electrons, resulting in a flux of hot electrons incident upon the surface from within. Subsequent inelastic scattering of the hot electrons by the adsorbed molecule (via a temporary negative ion shape resonance) provides a mechanism for redistributing energy from the hot electrons into the various degrees of freedom of the molecule [3–5]. If the energy placed into center-of-mass translational motion exceeds the relevant bond energy, then enhanced desorption (far beyond "thermal expectations") may occur. Here we report on recent developments both in conceptualizing and in theoretical modeling within the realm of hot electron femtochemistry at surfaces (HEFATS). First a closed form analytic expression for the resonance-assisted desorption rate induced by a broad band of laser-excited hot electrons is obtained. Second, a complementary method is proposed which involves a novel application of a metal-insulator-metal (M-I-M) tunnel junction [6] to produce a monochromatic, tunable electron flux internally incident upon the outer metal-vacuum interface, where the controlled HEFATS then occurs.

Within the Born-Oppenheimer limit, the total cross section for inelastic resonance scattering of hot electrons by a vibrationally active target is given by [3,7]

$$\sigma_{\text{tot}}(\varepsilon_{\text{in}}, \varepsilon; \tau_R = \hbar/\Gamma) \simeq \frac{\sigma_{\text{res}}}{4} \Gamma(\varepsilon_{\text{in}})\Gamma(\varepsilon_{\text{in}} - \varepsilon)$$
$$\times \left| \sum_{m=0}^{\infty} \frac{\langle \varepsilon | \tilde{m} \rangle \langle \tilde{m} | 0 \rangle}{\varepsilon_{\text{in}} - \varepsilon_a - \varepsilon_{\tilde{m}} + i\Gamma/2} \right|^2, \quad (1)$$

where ε_{in} is the energy of the incident electron, ε is the energy loss, $\Gamma(\varepsilon_{\text{in}})/\hbar$ [$\Gamma(\varepsilon_{\text{in}} - \varepsilon)/\hbar$] is the electron transition rate at the initial [final] energy into [out of] the resonance state, ε_a is the ("frozen nuclei") resonance energy, and $\langle \varepsilon | \tilde{m} \rangle$, etc., are translational/vibrational (T/V or V/V) overlap integrals, where $|\tilde{m}\rangle$ denotes vibrational states (with energy $\varepsilon_{\tilde{m}}$) of the negative ion-surface bond and $|\varepsilon\rangle$ is either a bound discrete or dissociative/desorptive continuum state of the neutral atom or molecule [7(a)]. The electron capture/scattering cross section $\equiv \sigma_{\text{res}}$ is evaluated at some appropriate fixed molecular geometry, yielding a slowly varying function of ε_{in} across the resonance which can be treated as a constant scale factor.

The desorption rate is expressed as the product of the cross section for inelastically scattering hot electrons from ε_{in} to $\varepsilon_{\text{in}} - \varepsilon$ (thereby exciting the center-of-mass motion associated with the bond to be broken) multiplied by $j'_{\text{el}}(\varepsilon_{\text{in}})$, the energy distribution of the hot electron flux incident upon the adsorbed molecule, integrated over the entire range of incident energy and over those energy losses in excess of D, the desorption energy; that is,

$$dN_{\text{des}}(\tau_R)/dt \simeq \int_D^{\varepsilon_{\text{max}}} \rho(\varepsilon) d\varepsilon$$
$$\times \int_{\varepsilon_{\text{min}}}^{\varepsilon_{\text{max}}} d\varepsilon_{\text{in}} j'_{\text{el}}(\varepsilon_{\text{in}})\sigma_{\text{Tot}}(\varepsilon_{\text{in}}, \varepsilon; \tau_R), \quad (2)$$

with $\rho(\varepsilon)$ the density of states for molecular T or V motion. In the case of photon-excited electrons, the limits $\varepsilon_{\text{max}} = \varepsilon_{\text{Fermi}} + h\nu$ and $\varepsilon_{\text{min}} = \varepsilon_{\text{Fermi}} + \varepsilon$ account for energy conservation and phase-space blocking imposed by the Pauli exclusion principle.

One of the most useful realizations of the resonant desorption process occurs in the "broad-band-excitation" limit [3,7(b),8]. Provided the photon energy is sufficiently above a desorption or channel threshold, this limit should be applicable to many of the experimental studies of laser-induced hot-electron desorption. If the variation with energy of j'_{el} is not too great over the width of the resonance, then an average value, say that at $\varepsilon_{\text{in}} \simeq \varepsilon_a$, can be used. Neglecting the explicit energy dependence of the level width functions [i.e., $\Gamma(\varepsilon_{\text{in}}) \approx \Gamma(\varepsilon_{\text{in}} - \varepsilon) \equiv \Gamma$], as

is common practice [3,7], the expression for the broad-band desorption rate which follows from Eqs. (1) and (2), upon ε_{in} integration with limits $\varepsilon_{\text{max}}(\varepsilon_{\text{min}}) \rightarrow +\infty(-\infty)$, takes the simple form

$$dN_{\text{des}}(\tau_R)/dt = (\pi/2)\langle j'_{\text{el}}\rangle \sigma_{\text{res}}(\hbar/\tau_R)\langle P_{\text{des}}(\tau_R)\rangle. \quad (3)$$

The total desorption probability per resonance event appearing in Eq. (3) is

$$\langle P_{\text{des}}(\tau_R)\rangle \equiv \int_D^{\varepsilon_{\text{max}}} \rho\, d\varepsilon \sum_{m,m'} \frac{S_{m,\varepsilon}S^*_{m',\varepsilon}}{1 + [(\varepsilon_{\tilde{m}} - \varepsilon_{\tilde{m}'})\tau_R/\hbar]^2}, \quad (4)$$

in terms of overlap integral products (equivalent to compound Franck-Condon factors) $S_{m,\varepsilon} \equiv \langle \varepsilon|\tilde{m}\rangle\langle \tilde{m}|0\rangle$, etc., as discussed at some length in conjunction with Eq. (19) and Fig. 8 in Ref. [3].

Both classical mechanics and semiclassical Gaussian wave-packet dynamics [9] provide insightful alternative formats for calculating $\langle P_{\text{des}}(\tau_R)\rangle$, as will now be shown. Initially, the desorbate is bound to the surface in the Gaussian vibrational ground state of $V_0(z)$, the molecule-surface potential energy curve associated with the electronic ground state of the system shown in Fig. 1. At some time defined as $t = 0$, a hot electron becomes trapped in the shape resonance responsible for the electron affinity level. The presence of this additional electron strengthens and compresses the molecule-surface bond [5]. This results in the potential energy curve labeled $V_{\text{exc}}(z)$ in Fig. 1. The displaced oscillator potential provides the forces acting upon the classical point mass or the Guassian wave packet representing the molecule translational motion. After a time delay $\Delta t > 0$, the trapped electron exits and the moving particle (wave packet) is returned to $V_0(z)$ displaced from its equilibrium position, possibly high enough up on the repulsive wall of V_0 to result in desorption,
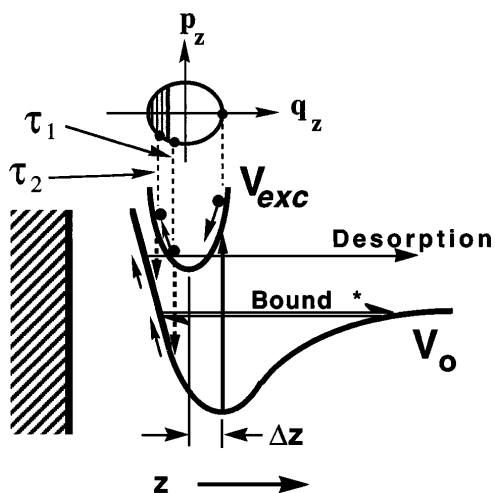
FIG. 1. Resonance-state phase-space trajectory (top) in relation to motion on real-space potential curves V_{exc} of the intermediate state and V_0 of the ground state. Return to V_0 at τ_1 results in bound state vibrational excitation whereas return at τ_2 results in excitation to the desorption continuum, where $\tau_1 < t_{\text{on}} < \tau_2 < T_{\text{vibe}}/2$.

as accounted for by a yet-to-be-determined distribution $=P_{\text{des}}(\Delta t)$, which is a function of the time delay spent on the displaced oscillator, negative-ion potential.

Under the near classical conditions appropriate to model systems such as NO/Pt, the periodic function $P_{\text{des}}(\Delta t)$ $[=P_{\text{des}}(\Delta t + T)$ with $T \Rightarrow T_{\text{vibe}} = 2\pi/\omega_0$, the vibrational period on $V_{\text{exc}}]$ is tolerably well represented by a top-hat structure switched on from $P_{\text{des}} = 0$ to $P_{\text{des}} = 1$ at $\Delta t = t_{\text{on}}(\Delta z)$ and back off at $\Delta t = T - t_{\text{on}}(\Delta z)$ (when Δz, the displacement of V_{exc} from V_0, exceeds ≈ 0.15 Å) [10]. The time interval between t_{on} and $T - t_{\text{on}}$ represents that part of the periodic phase-space trajectory, shown as the marked region at the top of Fig. 1, which returns the translational motion wave packet onto the desorptive wall of V_0. Formally, t_{on} is obtained from the solution of $p_z^2(t_{\text{on}})/2M + V_0(z(t_{\text{on}})) = D$, where both the momentum $p_z(t_{\text{on}})$ and the displacement $z(t_{\text{on}})$ have been acquired under the influence of V_{exc}, as suggested by the phase space trajectory in Fig. 1. In order to account for the continuous distribution of negative ion survival times (hence time delays above), $P_{\text{des}}(\Delta t)$ should be averaged over all delay times, weighted by the probability that the intermediate state is still populated at the given momentum when it is returned to the ground state [1(d),11]. This is given by the classical equivalent of Eq. (4), the desorption probability per resonance event, as

$$\langle P_{\text{des}}(\tau_R)\rangle = \frac{1}{\tau_R} \int_0^\infty d(\Delta t)e^{-\Delta t/\tau_R}P_{\text{des}}(\Delta t), \quad (5)$$

where an exponential survival probability, consistent with Lorentzian line shapes, has been adopted [8,11]. Invoking the periodic top-hat form for $P_{\text{des}}(\Delta t)$, the integral in Eq. (5) is straightforward and the resulting expression for the desorption yield is simply

$$\langle P_{\text{des}}(\tau_R)\rangle = \frac{\sinh([T - 2t_{\text{on}}(\Delta z)]/2\tau_R)}{\sinh(T/2\tau_R)}, \quad (6)$$

a very concise and manageable analytic solution to the resonant desorption process resulting from broad-band excitation.

With $\langle P_{\text{des}}(\tau_R)\rangle$ given by Eq. (6), the numerical consequences of Eqs. (3) and (6) are shown as dN_{des}/dt vs $\omega_0\tau_R$ plots in Fig. 2 for a range of values of t_{on} (hence Δz), as labeled, with the curves properly scaled with respect to each other. An initial increase in the desorption rate is obtained as the resonance lifetime increases from zero due to the displaced nuclear dynamics processes. It is apparent from Fig. 2 that smaller t_{on} or, equivalently, larger Δz hence larger intermediate state forces results in a larger desorption rate, all other things being equal. However, as the lifetime increases (perhaps due to increased barrier height or width, hence reduced electron barrier penetration probability), it follows from microscopic reversibility that the hot electrons cannot so easily enter the shape resonance and as a result, the desorption rate peaks and then decreases. It is interesting to note from Fig. 2 that the maximum
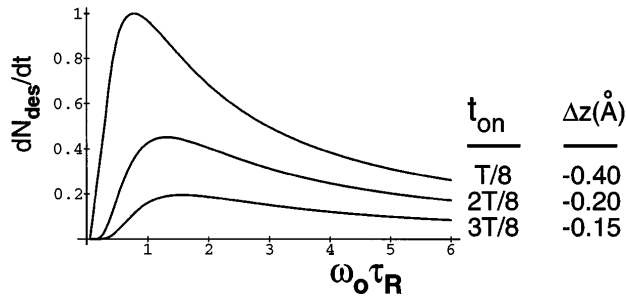
FIG. 2. Desorption rate (dN_{des}/dt) vs resonance lifetime resulting from broad-band excitation, as given by Eq. (3) with selected values of t_{on} (or Δz when V_{exc} is a harmonic potential with frequency ω_0), as labeled. While the absolute scale of the dN/dt axis is arbitrary, the curves are properly scaled with respect to each other.

FIG. 3. Potential energy diagram for the M-I-M HEFATS device.

desorption rate occurs when $\tau_R/T_{vibe} \simeq 0.1$–$0.2$. Since $\tau_R/T_{vibe} = \hbar\omega_0/\Gamma$, using experimentally known values of $\hbar\omega_0 \simeq 50$ meV and $\Gamma \simeq 0.5$ eV, it is observed that the values of the system parameters given to us by nature are in fact those values which are required for optimization of the phenomenon of resonance hot electron desorption.

Now consider the opposite limit, that of a tunable, narrow-band incident electron flux,

$$j'_{el}(\varepsilon_{in}) = j_0 \delta(\varepsilon_{in} - \varepsilon_\nu). \tag{7}$$

Again for expositional clarity, the classical picture of the nuclear dynamics is invoked, here allowing for replacement of the sum over interfering "m paths" connecting $|0\rangle$ with $|\varepsilon\rangle$ in Eq. (1) by a single classical path (with $m, m' \Rightarrow m_{class}$). The resulting desorption rate obtained from Eqs. (1), (2), (4), and (7) is

$$dN_{des}(\tau_R)/dt = \frac{j_0 \sigma_{res} \langle P_{des}(\tau_R)\rangle_{class}}{1 + [2(\varepsilon_\nu - \varepsilon_a)/\Gamma]^2}, \tag{8}$$

where $\langle P\rangle_{class}$ is obtained from Eq. (4) with the summation restricted to the single contribution $m = m' = m_{class}$. Accordingly, $\langle P\rangle_{class}$ is now invariant with τ_R, having lost the interference effects responsible for the τ_R dependence. Note that the energy $\varepsilon_{m_{class}}$ that appears in the denominator of Eq. (1) has now been incorporated into a renormalized value of ε_a.

An exciting new possibility in which electrons emitted from a M-I-M device are used to mediate femtochemical reactions at the outer metal-vacuum interface [6(b)] is shown in the potential diagram in Fig. 3. Typically the insulator and the top metal are of order 100 Å in thickness and the applied voltage V can be less than ϕ, the top metal work function, for HEFATS involving resonance states that are energetically unaccessible with external electron beams.

There are enough useful similarities between the relevant physics of the present device and that in BEEM (ballistic electron emission microscopy) [12] constructions so that the successful BEEM models can be used as templates for theoretical models of HEFATS with M-I-M sandwich structures. The essential feature is the adoption of an
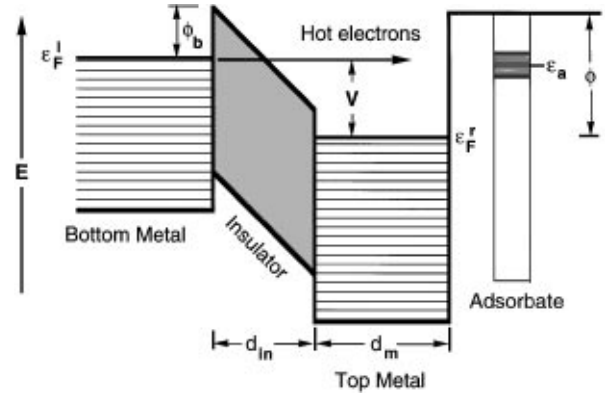
independent four-step model: (i) tunneling from bottom metal to tilted insulator conduction band [13]; (ii) transport through insulator, with possible phonon and polaron losses [14]; (iii) hot-electron transport and attenuation across top metal film [15]; (iv) resonant inelastic hot-electron scattering from adsorbates at top metal/vacuum interface [3]. From the theory of field emission tunneling [13] it is known that the energy distribution of the tunneling electrons shows a sharp Fermi edge and a width $\ll 0.1$ eV, for the fields ~ 0.02 V/Å experienced in the device. The total field emission current density into the insulator is given by the Fowler-Nordheim equation [13],

$$j_0(V; d_{in}) \simeq aF^2 \exp(-b\phi_b^{3/2}/F), \tag{9}$$

where $F = V/d_{in}$ (in V/Å), $a = (0.96 \times 10^{13}/\phi_b)e/$ sec V^2, $b = 0.683/$Å eV$^{1/2}$, and ϕ_b is the bottom metal-insulator barrier height. Phonon losses or broadening within the insulator are expected to be small [14]. A major effect is due to electron-hole pair excitation while traversing the top metal film [6(a)]. This is currently treated by introducing an exponential attenuation factor such that now the incident primary electron flux reaching the metal-vacuum interface is

$$j'_{el}(\varepsilon_{in}, V; d_{in}, d_m) \simeq j_0(V; d_{in}) \exp[-d_m/\lambda(\varepsilon_{in})]$$
$$\times \delta(\varepsilon_{in} - eV), \tag{10}$$

where $\varepsilon_\nu \equiv eV$, d_m is the metal thickness, $\lambda(\varepsilon_{in})$ is the electron attenuation length, and the small contribution due to secondary cascade electrons is omitted here.

The venerable theory of Quinn [15] gives a still-credible expression for γ, which in its simplest low-energy form is

$$\lambda(\varepsilon_{in}) \simeq \chi(r_s)(1 + \varepsilon_{in}/\varepsilon_{Fermi})^{1/2}/\varepsilon_{in}^2 \text{ Å}, \tag{11}$$

where the material-dependent $\chi(r_s) \simeq 10\,500/r_s^{7/2}$ eV^2 with r_s the usual Fermi-system electron density parameter. Taking Al("Cu") with $r_s \approx 2\,(3)$ as examples, Eq. (11) implies that $\lambda(\varepsilon_{in} = 3$ eV$) \approx 100\,(30)$ Å. The desorption/dissociation rate which follows from Eqs. (8)–(11) is a product of the absolute scale factors σ_{res} and $\langle P\rangle_{class}$, the resonance Lorentzian, and an electron source "window

function" composed of the exponentially competing, d_{in}-dependent field emission supply function, Eq. (9) (increasing with V), multiplied by the d_m-dependent top-metal attenuation (decreasing with V). The novel aspect of this structure is that by appropriate choice of device parameters ϕ_b, d_{in}, d_m, and r_s, one can produce an electron-source window spanning a chosen energy range of relevance to the particular femtochemical processes under consideration. A (normalized) set of window functions so obtained for an $r_s \sim 3$ metal is shown in Fig. 4(a), where systematic changes in window characteristics with metal thickness are apparent. The selective tuning into and detuning out of particular electron-attachment resonances ($\varepsilon_a = 2, 3, 4$ eV) is illustrated in Fig. 4(b) in the form of desorption rate as a function of applied voltage with system parameters as labeled. Certainly the promised tunability and selectivity in branching ratios between overlapping resonances (equivalently the chemical species) should be realizable with this M-I-M device.

In summary, two qualitatively different examples allowed highlighting some of the noteworthy characteristics of the HEFATS proposition. The first example considered the intermediate-negative-ion lifetime dependence in hot-electron-induced desorption stimulated by a broad-band distribution of incident electrons, typically found in ultrafast laser HEFATS. Conditions required for optimal desorption rates were established using the model presented here. An entirely new realization of HEFATS exploit-

ing the special tunability characteristics of a narrow-band energy distribution of incident electrons was proposed and some numerical consequences illustrating control of the bond-breaking desorption rate were presented. These examples can be regarded as indicators of the healthy progress towards the goal in which HEFATS is a standard tool in the arsenal of both the surface dynamicist and the femtochemist [16].
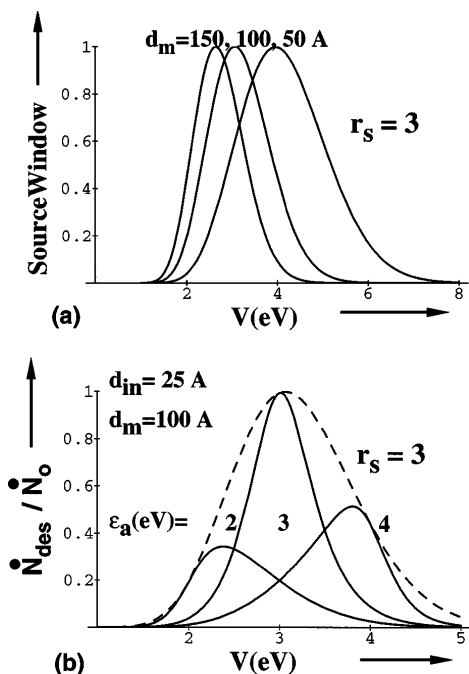
---

[1] (a) R. R. Cavanagh, D. S. King, J. C. Stephenson, and T. F. Heinz, J. Phys. Chem. **97**, 786 (1993); (b) *Laser Spectroscopy and Photochemistry on Metal Surfaces,* edited by H. L. Dai and W. Ho (World Scientific, Singapore, 1995); (c) X.-Y. Zhu, Annu. Rev. Phys. Chem. **45**, 113 (1994); (d) F. M. Zimmermann and W. Ho, Surf. Sci. Rep. **22**, 127 (1995).

[2] J. W. Gadzuk, in *Femtosecond Chemistry,* edited by J. Manz and L. Woste (VCH, Weinheim, 1995), p. 603.

[3] J. W. Gadzuk, Phys. Rev. B **44**, 13 466 (1991).

[4] R. E. Palmer and P. J. Rous, Rev. Mod. Phys. **64**, 383 (1992).

[5] (a) J. W. Gadzuk, L. J. Richter, S. A. Buntin, D. S. King, and R. R. Cavanagh, Surf. Sci. **235**, 317 (1990); (b) J. W. Gadzuk, Ref. [1(b)], p. 897; (c) J. W. Gadzuk, Surf. Sci. **342**, 345 (1995).

[6] (a) C. R. Crowell and S. M. Sze, Phys. Thin Films **4**, 325 (1967); H. Kanter, Phys. Rev. B **1**, 522 (1970); (b) R. G. Sharpe, St. J. Dixon-Warren, P. J. Durston, and R. E. Palmer, Chem. Phys. Lett. **234**, 354 (1995).

[7] (a) W. Domcke and L. S. Cederbaum, J. Phys. B **13**, 2829 (1980); N. S. Wingreen, K. W. Jacobsen, and J. W. Wilkins, Phys. Rev. B **40**, 11 834 (1989).

[8] H. J. Lipkin, Phys. Rev. B **46**, 15 534 (1992).

[9] (a) E. J. Heller, Acc. Chem. Res. **14**, 368 (1981); (b) D. J. Tannor and S. A. Rice, J. Chem. Phys. **83**, 5013 (1985); (c) J. W. Gadzuk, Annu. Rev. Phys. Chem. **39**, 395 (1988); (d) S. Y. Lee, W. T. Pollard, and R. A. Mathies, Chem. Phys. Lett. **163**, 11 (1989); (e) A. B. Myers, Chem. Phys. **180**, 215 (1994).

[10] This is essentially a statement that classical mechanics provides an adequate descritpion of the molecular dynamics throughout the round-trip curve switching, at least in the higher energy regime that applies for these displacements; see Ref. [5(c)].

[11] J. W. Gadzuk, J. Chem. Phys. **79**, 3982 (1983); A. R. Burns, E. B. Stechel, and D. R. Jennison, Phys. Rev. Lett. **58**, 250 (1987); F. M. Zimmermann and W. Ho, J. Chem. Phys. **100**, 7700 (1994).

[12] M. Prietsch, Phys. Rep. **253**, 163 (1995).

[13] J. W. Gadzuk and E. W. Plummer, Rev. Mod. Phys. **45**, 487 (1973).

[14] D. J. DiMaria and M. V. Fischetti, Appl. Surf. Sci. **30**, 278 (1987).

[15] J. J. Quinn, Phys. Rev. **126**, 1453 (1962).

[16] A. H. Zewail, J. Phys. Chem. **97**, 12 427 (1993); in *Femtochemistry,* World Scientific Series in 20th Century Chemistry (World Scientific, Singapore, 1994), Vols. I and II; *Femtosecond Chemistry* (Ref. [2]).

FIG. 4. (a) M-I-M electron-source window function vs applied voltage with $\phi_b \simeq 1$ eV and values of outer (Cu-like, $r_s \approx 3$) metal thickness d_m and other parameters as labeled. (b) Normalized desorption rate vs applied voltage for $\Gamma = 1$ eV resonance centered at $\varepsilon_a = 2, 3, 4$ eV. The dashed curve is the window function.